Life Sciences 231 (2019) 116539

Contents lists available at ScienceDirect

Life Sciences

journal homepage: www.elsevier.com/locate/lifescie

miR-21-5p promotes lung adenocarcinoma progression partially through targeting SET/TAF-Iα

Jiacheng Zhong[1], Xiaohu Ren[1], Zhihong Chen, Hang Zhang, Li Zhou, Jianhui Yuan, Ping Li, Xiao Chen, Wei Liu, Desheng Wu, Xifei Yang, Jianjun Liu*

Institute of Toxicology, Shenzhen Center for Disease Control and Prevention, No 8 Longyuan Road, Nanshan District, Shenzhen 518055, Guangdong, China

ARTICLE INFO

Keywords:
Lung adenocarcinoma
miR-21-5p
SET/TAF-Iα

ABSTRACT

Objective: Although SET(I2PP2A) and miRNAs are reported to play a pivotal role in lung cancer, the underlying mechanisms have remained obscure. To address this issue, we investigated how miRNAs and SET participate in the progression of lung cancer.

Methods: miRNAs that target SET were predicted from multiple miRNA databases. Three human NSCLC cell lines and two normal lung cell lines were used to evaluate aberrant miRNA and SET expressions. A dual luciferase reporter assay system was employed to verify the interaction between miRNA and SET. Stable miRNA knockdown and SET overexpression in A549 cells were achieved through lentivirus transfection; the corresponding influences on lung cancer progression were also examined.

Results: In this study, A549 was the sole cell line to lack SET/TAF-Iα expression, which was inversely correlated with the up-regulation of miR-21-5p. SET was subsequently revealed as the direct target site of miR-21-5p in A549 cells. The stable miR-21-5p knockdown and SET/TAF-Iα overexpression were shown to markedly enhance the expression of SET/TAF-Iα and to inhibit the migration, invasion, proliferation as well as the *in vivo* tumorigenicity of A549 cells.

Conclusion: We suggest that SET/TAF-Iα might be a tumor suppressing factor regulated by miR-21-5p in lung adenocarcinoma. This might provide a target for lung adenocarcinoma therapy.

1. Introduction

Lung cancer is a highly heterogeneous malignancy and leading cause of worldwide cancer death [1]. Nearly one-quarter of cancer-related deaths in the USA are estimated to be associated with lung cancer [2]. Non-small-cell lung cancers (NSCLC) are responsible for the largest proportion of newly diagnosed lung cancer cases; they are composed of three tumor classes, including adenocarcinoma, squamous cell carcinoma along with large cell carcinoma, among which the morbidity of lung adenocarcinoma is the highest [3]. Different from lung squamous carcinoma, which is generally connected with tobacco smoking, lung adenocarcinoma is highly incidental in non-smokers as well [4].

SET was first recognized as a SET-CAN fusion gene in a case of acute undifferentiated leukemia [5]; it can be also termed protein phosphatase 2A inhibitor, I2PP2A [6] or template-activating factor-I, TAF-I [7], depending on the corresponding functions. In addition, SET was also reported to modulate the DNA-damage response (DDR) of chromatin-associated double-strand breaks (DSBs) [8] and is essential for sister chromatid segregation in oocyte meiosis II [9]. SET comprises two isoforms, the longer isoform TAF-Iα and the shorter one, TAF-Iβ. While numerous studies have focused on the critical roles of TAF-Iβ, including acetylation inhibitor [10] and histone chaperone [11], the potential of TAF-Iα remains poorly illustrated. Aside from the diversity of regulating functions, SET exists at elevated levels in many cancers, such as breast cancer [12] and pancreatic cancer [13]. Notably, SET was found to be a therapeutic target of the sphingosine analogue drug FTY720 in lung tumors [14].

MicroRNAs (miRNAs) are a class of small noncoding RNA molecules of ~22 nucleotides [15] that induce translational inhibition or post-transcriptional mRNA degradation by binding to the 3′-untranslated regions (3′UTRs) of target mRNAs [16]. Aberrant miRNA expression has been reported in many cancers, including lung cancer. With the potential of miRNAs as stratifying the specific subtype [17], evaluating the course of disease [18], or estimating the response of treatment [19]

* Corresponding author at: Institute of Toxicology, Shenzhen Center for Disease Control and Prevention, No 8 Longyuan Road, Nanshan District, Shenzhen 518055, China.
E-mail address: junii8@126.com (J. Liu).
[1] These authors contributed equally to this work.

https://doi.org/10.1016/j.lfs.2019.06.014
Received 18 March 2019; Received in revised form 29 May 2019; Accepted 5 June 2019
Available online 06 June 2019
0024-3205/

being deeply exploited in lung cancer, understanding of miRNA downstream targets is in rising demand.

Collectively, both SET and miRNAs have been identified as important players in lung cancer. A previous report indicated that miR-502-3p could suppress the malignancy of hepatocellular carcinoma through regulating SET [20]. To advance insight into the potential interaction between miRNA and SET in lung cancer, which is currently not reported, we designed and conducted a series of research studies. The combined utilization of multiple miRNA databases, including miRWalk, miRDB, TargetScan and miRanda, predicted that miR-21-5p, miR-23a-3p and miR-199b-5p targeted SET. In the present study, miR-21-5p was found to be significantly upregulated in A549 cells and was therefore chosen for in-depth investigation. We find that stable miR-21-5p knockdown and SET/TAF-Iα overexpression significantly inhibits cell migration, invasion, proliferation, and *in vivo* tumorigenicity of A549 cells, while the results of Western blot analysis show enhanced SET/TAF-Iα expression in A549 cells induced by stable miR-21-5p knockdown or SET/TAF-Iα overexpression. This suggests that miR-21-5p might be involved in the pathogenic processes of lung adenocarcinoma partially through targeting SET/TAF-Iα. Taken together, these observations might provide evidence for a novel therapeutic target of lung adenocarcinoma.

2. Materials and methods

2.1. Cell lines and reagents

The human squamous carcinoma cell lines SW-900, NCI-H520 and human lung adenocarcinoma cell line A549 were purchased from the American Type Culture Collection. The human bronchial epithelial cell line BEAS-2B and human embryonic lung cell line WI-38 were obtained from the China Center for Type Culture Collection. RPMI 1640, DMEM culture medium, fetal bovine serum (FBS), penicillin–streptomycin and trypsin were purchased from Gibco (Carlsbad, USA). Primary mouse monoclonal antibodies against SET (sc-133138), β-actin (sc-47778) and rabbit polyclonal antibody against Cyclin D1 (sc-718), were purchased from Santa Cruz Biotechnology (Dallas, USA), and rabbit monoclonal antibody against MMP-9 (ab137867) was purchased from Abcam (Cambridge, UK), Anti-mouse and anti-rabbit secondary antibody were purchased from Invitrogen (Carlsbad, USA).

2.2. Cell culture

A549 cells were cultured and maintained in DMEM medium and SW-900, NCI-H520 and BEAS-2B cells were cultured and maintained in RPMI 1640 medium, both media containing 10% FBS, 100 μg/ml penicillin and 100 μg/ml streptomycin, Cells were incubated at 37 °C in 5% CO_2.

2.3. RNA isolation and analysis

Total RNA of cultured cells was isolated using TRIZOL reagent (Invitrogen). Reverse transcription was performed by miScript II RT PCR (QIAGEN, Germany). qRT-PCR for miRNA measurement was subsequently performed by miScript SYBR Green PCR Kit (QIAGEN) miRNA expression was normalized to U6 small nucleolar RNA. All RT-qPCR reactions were repeated in triplicate and the $2^{-\Delta\Delta Ct}$ method was utilized for analysis. The following primers were used for quantification:

miR-199b-5p-F:5′-AGTCCCAGTGTTTAGACTATCTG-3′,
miR-21-5p-F:5′-CACGTAGCTTATCAGACTGATG-3′,
miR-23a-3p-F:5′-CATCACATTGCCAGGGATTTC-3′,
hsa-U6-F:5′-CTCGCT TCGGCAGCACA-3′,
hsa-U6-R:5′-AACGCTTCACGAATTTGCGT-3′

The universal primer available at miScipt SYBR Green PCR Kit served as the reverse primer for each miRNA aside from internal control, U6 small nucleolar RNA. Q-PCR was performed under the following amplification conditions: one cycle at 95 °C for 15 min followed by 40 three-step cycles including 15 s at 94 °C for denaturation, 30s at 55 °C for annealing and 34 s at 70 °C for extension.

2.4. Western blot analysis

Cells grown in culture flasks were washed with PBS to remove the residual culture medium and the total cell protein was extracted in individual flasks with 200 μl Cell lysis buffer for Western and IP (Beyotime, China). The protein concentration of each cell lysate was determined with a BCA kit (Thermo Fisher Scientific, USA) and adjusted to be equal before the supernatant was mixed with a corresponding volume of 4 × sample loading buffer and placed in boiling water bath for 10 min. SDS-PAGE gel comprised 10% separating gel and 5% stacking gel was used to separate denatured total protein. Semi-Dry blotter (Bio-rad, USA) was employed to electrically transfer the separated protein to a polyvinylidene difluoride membrane (PVDF). The membranes were blocked for 2 h at RT before being incubated in TBST containing primary antibodies (1:1000) at 4 °C overnight. The following day, the membranes were washed with TBST before incubation with secondary antibody (1:5000) at RT for 1 h. The membranes were washed again and visualized with Supersignal West Dura Extended Duration Substrate (Thermo scientific) in ECL™ Western blotting detection system (ImageQuant™ RT, GE Healthcare). The Western blot bands were subjected to gray value analysis by ImageJ. The relative intensity of each protein band was normalized to the corresponding β-actin expression.

2.5. Stable miR-21-5p knockdown in A549 cells

The inhibitory RNA expression cassette (Tough Decoy cassettes, TuD) targeting miR-21-5p was designed according to the optimized conditions described in a previous report [21]. The corresponding sequence incorporating EcoR I and BamH Isites was synthesized by General Biosystems (Anhui, China):

GGACGAGGATCCGGCGCTAGGATCATCAAC**TCAACATCAGTC**<u>**ATC**</u>
<u>**T**</u>**TGATAAGCTA**CAAGTATTCTGGTCACAGAATACAAC**TCAACATCAGT**
C<u>**ATCT**</u>**TGATAAGCTA**CAAGATGATCCTAGCGCCACCTTTTTTGAAT
TCT.

The nucleotide base shown in bold represents the miRNA-binding site (MBS) for miR-21-5p; the underlined 4-nt insertion was intended for averting RISC cleavage and enhancing the inhibitory efficiency [21]. The foregoing synthetic nucleotide sequence underwent endonuclease digestion with EcoR I and BamH I. Then, the desired sequence for inhibitory RNA expression cassette was cloned into the multiple cloning site of plvx-shRNA2-Puro lentiviral vector. The resulting constructions were verified by DNA sequencing; recombinant vector packaging was performed in HEK-293T cells. After 2d of transfection, HEK-293T cells were digested, cell debris was removed by centrifugation at 4 °C, 4000*g* for 12 min. Cell supernatant was harvested and centrifuged with a 0.45 μm filter membrane at 4 °C, 50,000*g* for 2 h before lentiviral particles were collected and dissolved in PBS for later use. A549 cells at logarithmic phase were applied to lentivirus transduction about 24 h post-transfection; culture media containing 1 μg/ml puromycin was used to eliminate the uninfected cells for up to 7 days; knockdown efficiency was determined by Q-PCR analysis with the previously described miR-21-5p and U6 primer. The stable miR-21-5p knockdown A549 cells were named A549-TuD21 cells and passaged for follow up assays.

2.6. Stable SET/TAF-Iα overexpression in A549 cells

Forward primer and reverse primer of SET/TAF-Iα were designed

according to the CDS of SET transcript variant 1 (NCBI Reference Sequence: NM_001122821. 1) with the restriction enzyme sites of EcoR I and BamH I being introduced:

SET-F(EcoRI):5′-GGAATTCGTGGTCTGGTTCTGGGACTTC-3′
SET-R(BamHI):5′-CGGGATCCGAAGGTTGGAATCCATCAGTGTTC-3′

The primers were synthesized by Sangon Biotech (Shanghai, China), total RNA of human L-02 cells was extracted, reverse transcription was performed to produce cDNA as template for SET/TAF-Iα amplification. pCDH-CMV-MCS-EF1-Puro was used as transfection vector while EcoR I-BamH I was used as cloning strategy. The recombinant vector was packaged and transfected into A549 cells in accordance with the approach for constructing A549-TuD21. The successfully constructed SET/TAF-Iα overexpression A549 cells were named A549-SET and underwent RT-qPCR verification by utilizing the following primer pairs:

SET/TAF-Iα-F:5′-AGAGCTTCTTTACCTGGTTTACTGAC-3′
SET/TAF-Iα-R:5′-CATCATCCATATCGGGAACCAAGTAG-3′
β-Actin-F:5′-CATGTACGTTGCTATCCAGGC-3′
β-Actin-R:5′-CTCCTTAATGTCACGCACGAT-3′

2.7. Dual luciferase reporter assay

The binding site between miR-21-5p and SET 3′-UTR was located by Web-based bioinformatic target gene predictions (http://www.targetscan.org/). The sequences of SET 3′-UTR with or without a scrambled miR-21-5p binding site were designed and synthesized by Sangon Biotech (Shanghai, China) before being cloned at the 3′-end of Renilla luciferase in psiCHECK-2 vector. XhoI + NotI was used as cloning strategy. Recombinant plasmid psicheck2-SET-3′UTR (W) or psicheck2-SET-3′UTR (M) were transfected into adherent A549 or A549-TuD21 cells by lipofectamin 2000 (Thermo Fisher Scientific), respectively. The cells from four experimental groups were then lysed by passive lysis buffer 48 h post-transfection. Luciferase activities were measured using Dual-Luciferase Reporter Assay System (Promega, USA) with gloMax luminometer (Promega); the Firefly luciferase activities were normalized against the Renilla luciferase. The experiment was performed in triplicate independently.

2.8. In vitro scratch assay

Cell migration was estimated by vitro scratch assay. A549, A549-TuD21 and A549-SET cells were seeded into 6-well plates and cultured until confluent monolayers were formed. An artificial gap was created in each well by the vertical scratch of a 200 μl pipette tip. After cell debris were thoroughly washed out by PBS, the scratched cells were then subjected to further culture for up to 24 h. Image acquisition was performed with a digital camera system; the width of the gap was measured using Image-Pro Plus 6.0 software and analyzed statistically.

2.9. Transwell matrigel invasion assay

Each well of 24-well Transwell plate (Invitrogen) was carefully covered by matrigel (BD Biosciences, USA) prior to the experiment. The prepared plates were used for assessing the cell invasion. The densities of suspended A549, A549-TuD21 and A549-SET cells were adjusted respectively to 5×10^5 cells/ml with serum free medium; 100 μl of cell suspensions were pipetted to the upper level of the chamber while the lower well was supplemented with 500 μl of culture medium containing 10% FBS. The incubation lasted 24 h at 37 °C in 5% CO_2, the remaining uninvaded cells on the upper level were scraped off, while the invaded cells were fixed with methanol for 10 min and stained with 0.1% crystal violet solution. The invaded cells in three randomly selected fields were photographed at 100× magnification and counted.

2.10. Cell proliferation assay

Cell proliferation was determined using Cell Counting Kit-8 (Dojindo Molecular Technologies, Japan). Briefly, A549, A549-TuD21 and A549-SET cells were suspended in serum-free medium containing 10% CCK-8 solution. Prepared cell suspensions were seeded in 6 replicates at densities of 1×10^3 cells per well in 96-well flat-bottom plates (Corning, USA). The incubation was sustained for up to 72 h. Serum-free medium containing the same proportion of CCK-8 was used as a blank control. The absorbance at 450 nm of each well was measured every 24 h to evaluate cell proliferation.

2.11. Tumorigenicity assay in nude mice

Fifteen female Balb/c nude mice aged between 4 and 5 weeks were purchased from Vital River Laboratory Animal Technology Co., Ltd. (Beijing, China). Animals were maintained under specified-pathogen-free (SPF) condition in the Animal Experimental Center at Shenzhen Center for Disease Control and Prevention (Shenzhen, China). All experiments were performed in compliance with the standard operating procedures of the local Ethics Committee. A total of 1.5×10^7 A549 cells, along with equal number of A549-TuD21 and A549-SET cells in logarithmic growth phase, were collected with pancreatin–EDTA. A suspension of approximately 3×10^6 cells in 0.3 ml was seeded into the right flank of nude mice through subcutaneous injection; 4 weeks later, the tumor-bearing nude mice were killed by CO_2 and the tumor tissues were collected.

2.12. Flow cytometry analysis

A total of 1×10^6 A549/A549-TuD21/A549-SET cells was detached and collected from culture flasks, washed twice with 1 ml PBS wash buffer, and resuspended. For cell cycle analysis, cells were treated with 1 ml DNA staining solution and 10 μl permeabilization solution. Cells were vortexed for 10s vortex and the reaction incubated in the dark at RT for 30 min prior to flow cytometry analysis. Flow cytometry analysis was performed using a BD Accuri C6 Flow Cytometer and data was analyzed using FlowJo.

2.13. Statistical analysis

Data were analyzed using Graphpad prism 5 statistical software. Two-tailed paired *t*-test and one-way ANOVA were conducted to determine the statistical significance. The data are presented as mean ± standard deviation. Results with a p-value < 0.05 were considered statistically significant.

3. Results

3.1. A549 cells lacking SET/TAF-Iα expression accompanied by upregulated miR-21-5p as compared to NCI-H520, SW 900 and BEAS-2B cells

To gain insight into the interaction between miRNAs and SET, multiple miRNA prediction databases grounded in complementary base pairing rule between miRNAs and their target genes, as well as the locating features of miRNA binding sites, including miRWalk, miRDB, TargetScan and miRanda, were used to predict the potential miRNAs targeting SET. These databases jointly identified three miRNAs, including miR-21-5p, miR-23a-3p and miR-199b-5p, that could possibly target SET. To lay a foundation for in-depth study, we performed a screening test based on RT-qPCR to quantify the expression of three predicted miRNAs in different cell lines, involving lung adenocarcinoma cell A549, human squamous carcinoma cell SW-900, NCI-H520, human bronchial epithelial cell BEAS-2B and human embryonic lung cell WI-38. The cancer cell line with the most significant miRNA

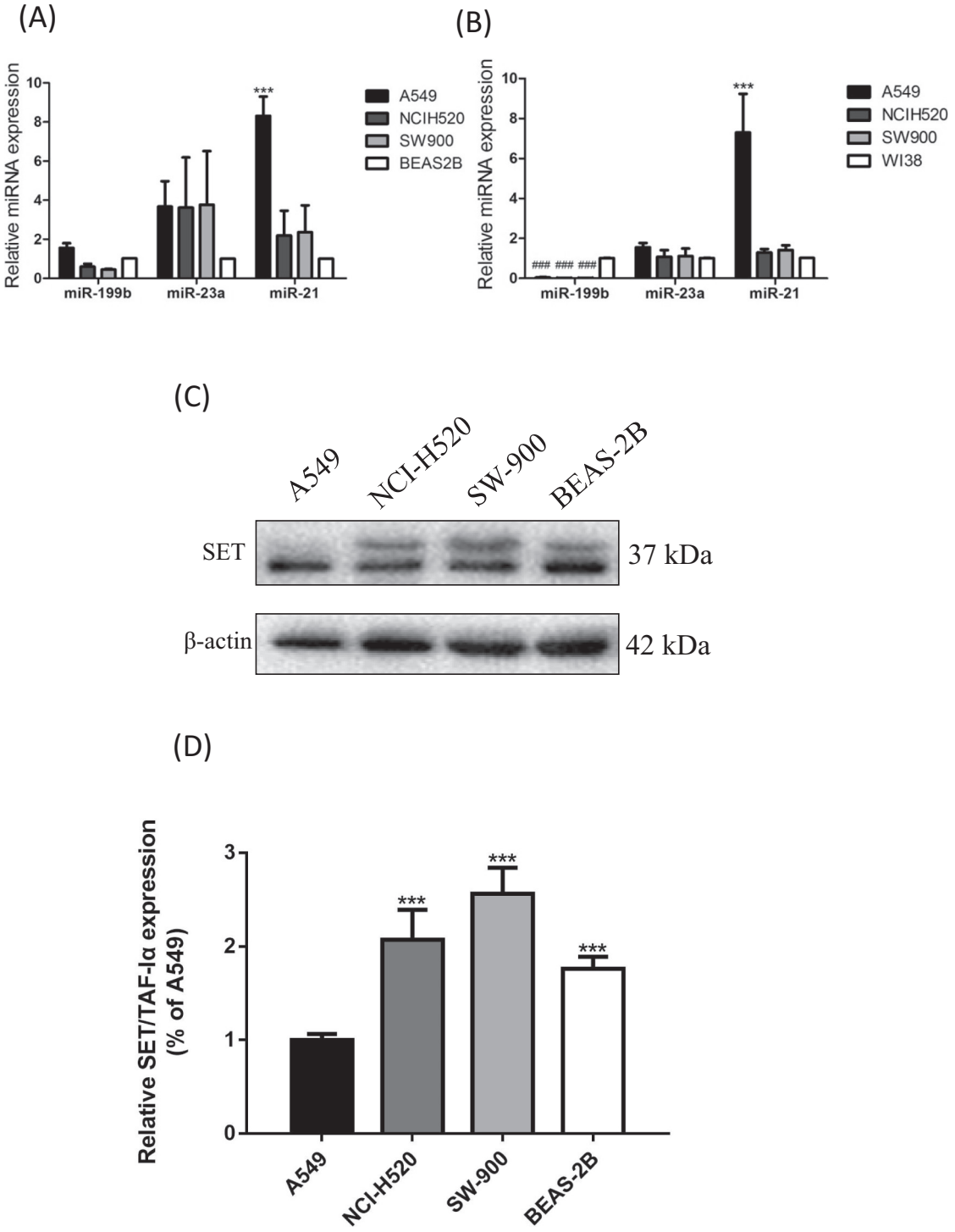

Fig. 1. A549 cells overexpress miR-21-5p and lack SET/TAF-Iα expression. The relative expression of miR-21-5p, miR-23a-3p and miR-199b-5b were measured by RT-qPCR in lung cancer and normal cell lines. Results were analyzed and depicted by normalizing relative miRNA expression to that of BEAS-2B cells (A) or WI-38 cells (B). All values are expressed as mean ± SD, $^{***}p < 0.001$ *versus* BEAS-2B cells, $^{###}p < 0.001$ *versus* WI-38 cells. A representative Western blot is shown (C) along with the analysis of SET/TAF-Iα protein expression (D). The data are represented as mean ± SD, $^{***}p < 0.001$ of at least three independent experiments, SET/TAF-Iα expressions are normalized to internal control β-actin.

variation *versus* normal lung cell lines, which indicated stronger potential interaction between miRNA and SET, was selected for further investigation. In the result of RT-qPCR (Fig. 1A, B), the relative miRNA expression by normalizing against either BEAS-2B or WI-38 demonstrated that miR-21-5p was significantly upregulated in A549 cells as compared to both NCI-H520 and SW-900 cells. Notably, a nearly 8-fold increase of miR-21-5p expression was detected by comparing A549 cells against BEAS-2B cells, which was more remarkable than WI-38 (nearly 7-fold increase). BEAS-2B cells were therefore selected as the normal cell control in Western blot analysis. There were no significant variations of miR-23a being detected, nevertheless, we found that miR-199b expression was relatively low in cancer cells as compared to normal control cells. Since the robust miR-21-5p expression might influence target gene expression, we performed Western blot analysis to

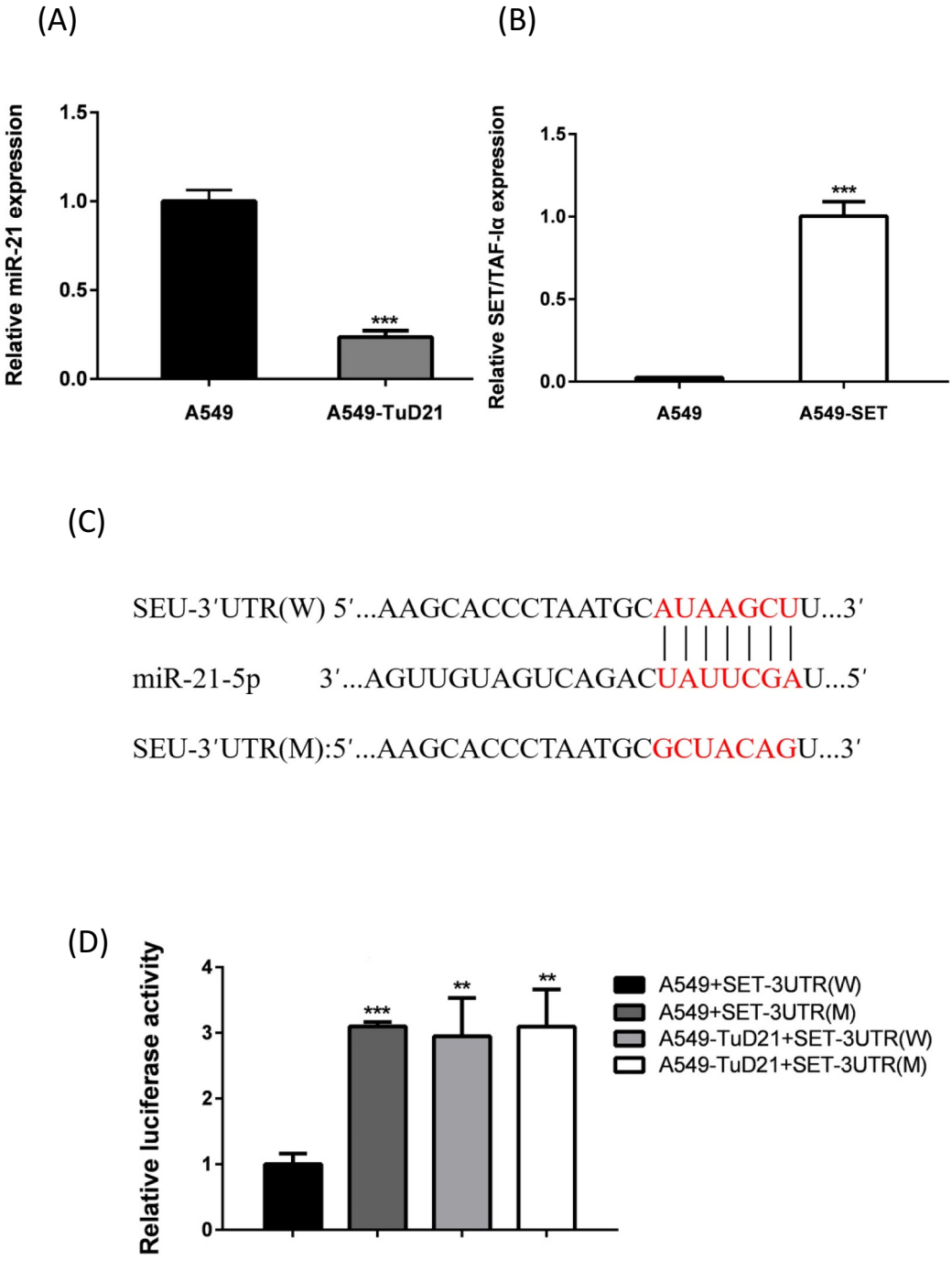

Fig. 2. Verification of stable miR-21-5p knockdown (A) and SET/TAF-Iα overexpression (B) in A549 cells with RT-qPCR. The data show the mean ± SD of three independent experiments, $^{***}p < 0.001$ compared with A549 cells. The diagram (C) of the luciferase reporter containing the wild-type or mutant miR-21-5p binding sequence in the 3′-UTR of SET mRNA: the successfully constructed A549-TuD21 cells were applied to dual luciferase reporter assay (D), the columns represent relative luciferase activities by normalizing *Renilla* luciferase activities to corresponding firefly luciferase activities, the data represent mean ± SD, $^{**}p < 0.01$ and $^{***}p < 0.001$ *versus* A549 cells transfected with luciferase reporter vector containing wildtype SET 3′-UTR of three independent experiments.

investigate miR-21-5p-associated regulation upon SET at the protein level. As depicted in (Fig. 1C), Western blot analysis showed that A549 was the only cell line to lack SET/TAF-Iα expression among the four tested cell lines, including both lung squamous carcinoma cells and normal lung bronchial epithelial cells. This result suggested that the aberrant expression of SET/TAF-Iα in A549 cells might be a specific characteristic for lung adenocarcinoma.

3.2. Stable miR-21-5p knockdown and SET/TAF-Iα overexpression in A549 cells

The results of RT-qPCR and Western blot assay suggested that A549 cells overexpress miR-21-5p and lack SET/TAF-Iα expression. To further explore the potential mechanism underlying this correlation, stable miR-21-5p knockdown and SET/TAF-Iα-overexpressed A549 cells were constructed as described previously. To verify the efficacy of lentivirus-mediated endogenous miR-21-5p inhibition and SET/TAF-Iα overexpression, we performed qRT-PCR analyses involving A549 cells

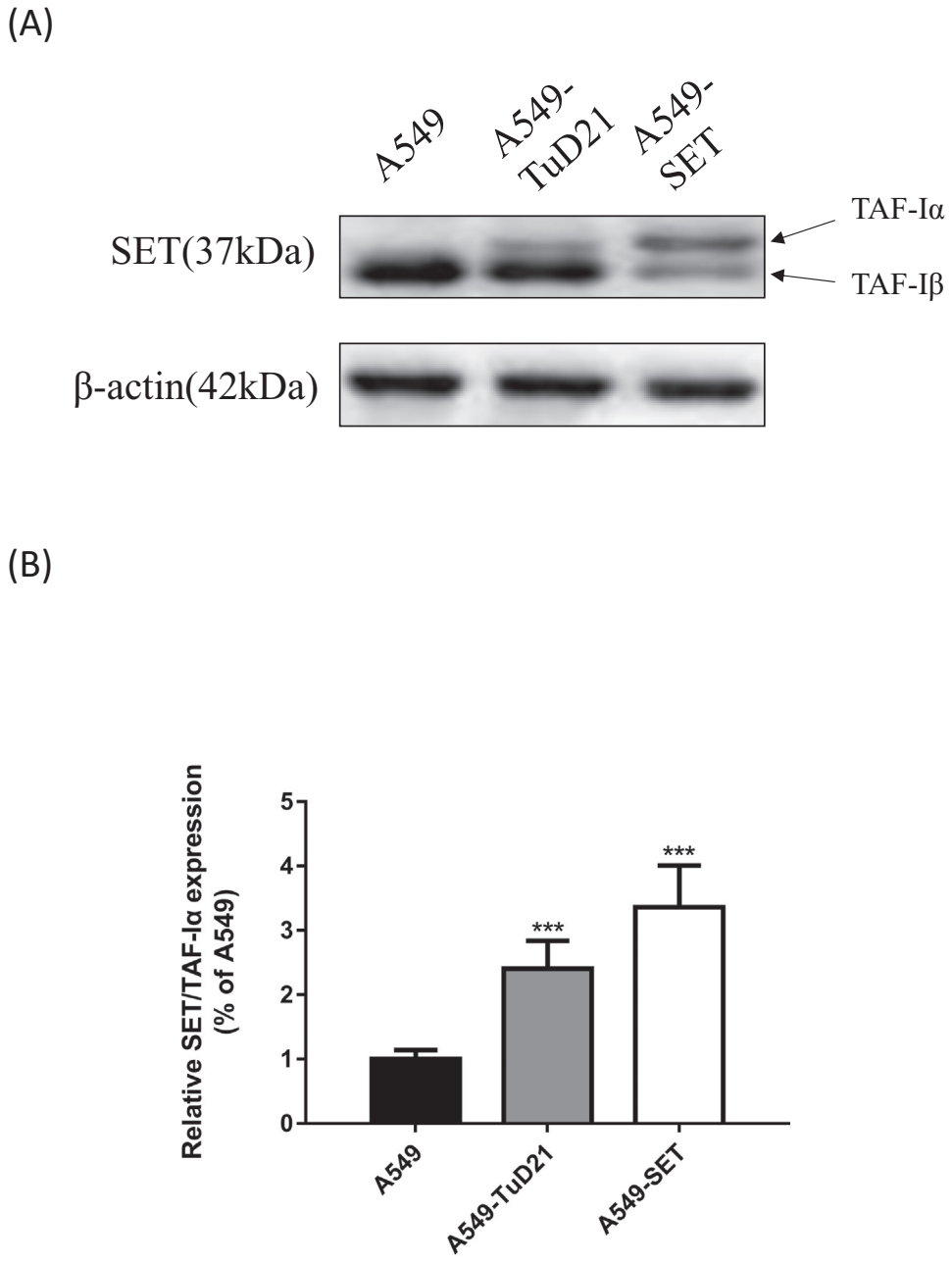

Fig. 3. The representative Western blots of SET/TAF-Iα involving A549, A549-TuD21 and A549-SET cells are shown in (A), the result analysis (B) indicated that stable miR-21-5p knockdown and SET/TAF-Iα overexpression enhanced the SET/TAF-Iα expression in A549 cells, all of the values are expressed as mean ± SD, $^{***}p < 0.001$ and the experiments were repeated three times.

accompanied by either A549-TuD21 or A549-SET cells. The results showed that miR-21-5p expression in A549-TuD21 cells was reduced by approximately 70% (Fig. 2A) while SET/TAF-Iα was nearly 10-fold overexpressed (Fig. 2B) in A549-SET cells as compared to A549 cells. These data demonstrated successful and stable miR-21-5p knockdown and SET/TAF-Iα overexpression in A549 cells.

3.3. SET is the direct target site of miR-21-5p in A549 cells

The 3′-UTR of exogenous gene SET was cloned to the downstream of Renilla luciferase. We transfected A549 or A549-TuD21 cells with luciferase vectors containing sequences of SET 3′-UTR with or without miR-21-5p binding sites being scrambled, respectively. Luminometer results were analyzed (Fig. 2D) and showed that the relative luciferase activity of A549 cells transfected with wildtype SET 3′-UTR was significantly reduced as compared to other experimental groups (either with SET 3′-UTR mutated or miR-21-5p knocked-down). These data further verified the interaction between miR-21-5p and SET 3′-UTR in A549 cells.

3.4. Stable miR-21-5p knockdown and SET/TAF-Iα overexpression enhanced SET/TAF-Iα expression in A549 cells

As an oncoprotein, SET participated in many physiological or pathological processes. Based on the verification by the dual luciferase reporter system, we hypothesized the alterations of SET expression at the protein level would occur in A549-TuD21 cells. Western blot analysis involving A549, A549-TuD21 and A549-SET cells showed that SET/TAF-Iα was enhanced in both A549-TuD21 and A549-SET cells (Fig. 3A), which confirmed the successful forced overexpression of SET/

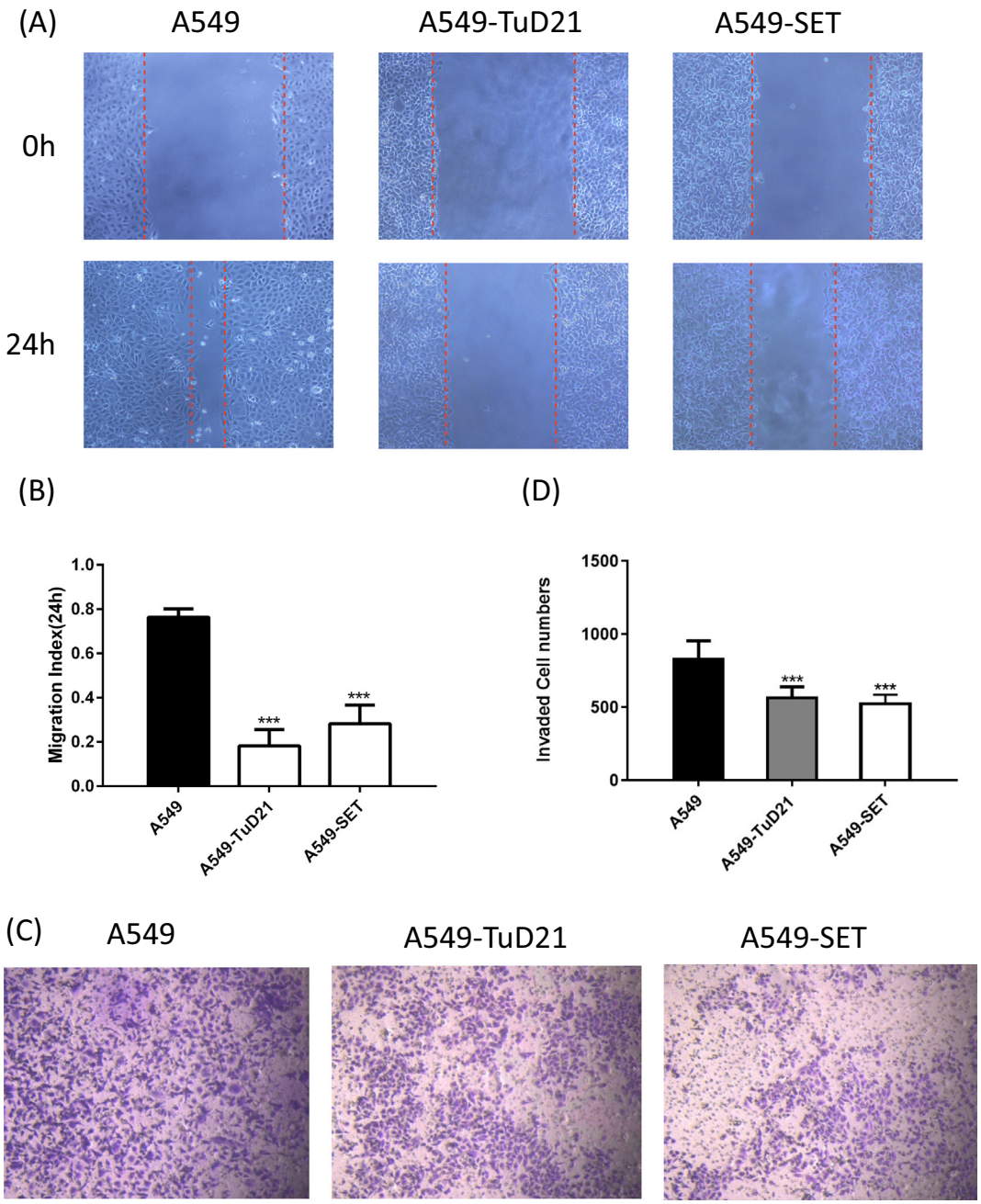

Fig. 4. Stable miR-21-5p knockdown and SET/TAF-Iα overexpression significantly inhibit cell proliferation, migration, invasion and *in vivo* tumorigenesis of A549 cells. Representative images of straight wound area were acquired in each culture well at 0 h and 24 h (A) and analyzed (B). The columns represent the migration index for each kind of cell expressed as a value relative to the distance moved by the cell monolayer. The invasion of A549, A549-TuD21 and A549-SET cells was examined using the transwell system, the representative images are presented (C). After 24 h treatment with matrigel, the number of successfully invading A549, A549-TuD21 and A549-SET cells was counted (D). Growth curves of A549 and A549-TuD21 and A549-SET cells were measured with CCK8 assay (E). The foregoing experiments were repeated at least three times. The tumor-bearing mice were terminated after a 4-week observation period (F), and the tumor weight was measured and calculated (G). The data are presented as mean ± SD, $p < 0.05$, $^{***}p < 0.001$ as compared with A549 cells.

TAF-Iα in A549 cells (A549-SET) and suggested the degradation or repression of SET/TAF-Iα at the transcriptional level might be attenuated due to the knockdown of miR-21-5p (A549-TuD21).

3.5. Stable miR-21-5p knockdown and SET/TAF-Iα overexpression significantly inhibits cell migration, invasion and proliferation of A549 cells

To evaluate the potential effect of stable miR-21-5p knockdown or SET/TAF-Iα overexpression on the migration of A549 cells, an *in vitro* scratch assay was applied to assess cell migration capability. As depicted in (Fig. 4A), 24 h after scratch induction, cell migration was significantly inhibited in A549-TuD21 and A549-SET cells compared with A549 cells. Transwell matrigel invasion assay showed that A549-TuD21 and A549-SET cells exhibited decreased cell invasion as compared to A549 cells (Fig. 4C). Cell proliferation was measured by CCK-8 assay. As shown in (Fig. 4E), when compared to A549 cells, the proliferation of A549-TuD21 and A549-SET was significantly suppressed after 48 h of culture.

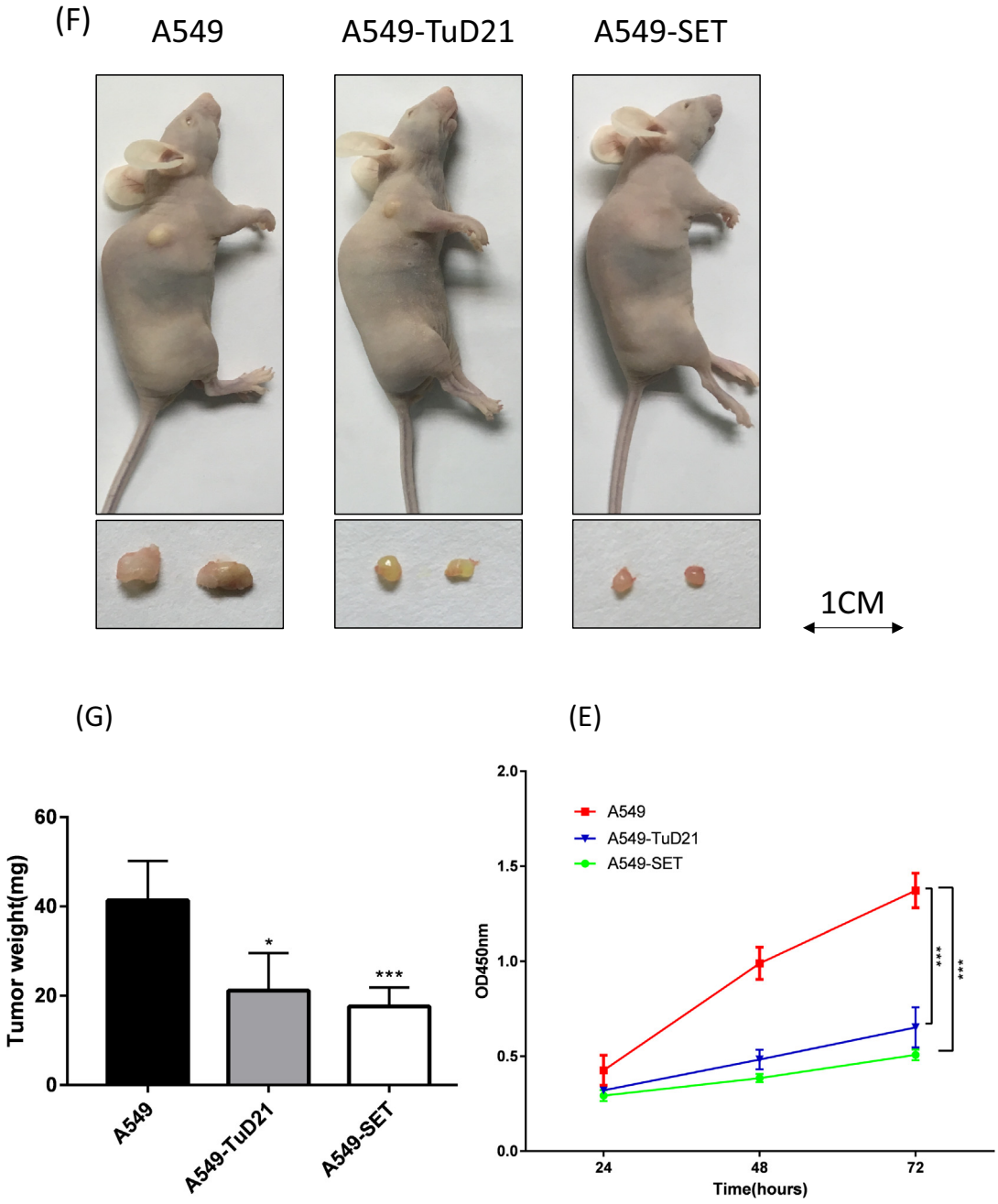

Fig. 4. (*continued*)

3.6. Stable miR-21-5p knockdown and SET/TAF-Iα overexpression suppresses the in vivo tumorigenicity of A549 cells

A xenograft tumor model was used to clarify whether miR-21-5p knockdown and SET/TAF-Iα overexpression could also influence the *in vivo* tumorigenicity of A549 cells. Tumor-bearing mice were terminated after a 4-week observation period (Fig. 4F), the tumor or mass isolated, weighed and measured. Quantitation of tumor weight for tumorigenesis evaluation in tumor-bearing nude mice is shown in Fig. 4G.

3.7. Stable miR-21-5p knockdown and SET/TAF-Iα overexpression lead to arrest of cell-cycle transition in the G0/G1 phase

A549, A549-TuD21 and A549-SET cells were subjected to flow cytometry analysis to evaluate the effects of miR-21-5p knockdown and SET/TAF-Iα overexpression on cell cycle distribution, Compared to A549 cells, the proportion of A549-TuD21 and A549-SET cells in the G0/G1 phase increased significantly, indicating that stable miR-21-5p knockdown and SET/TAF-Iα overexpression caused arrest of the cell cycle transition of A549 cells in the G0/G1 phase (Fig. 5A); this might contribute to the inhibited A549 cell malignancy.

3.8. Stable miR-21-5p knockdown and SET/TAF-Iα overexpression suppress expression of MMP-9 and Cyclin D1 in A549 cells

Given the significant inhibitory effect of miR-21-5p knockdown and SET/TAF-Iα overexpression on multiple oncogenic functions of A549 cells, the parameters associated with invasion and migration (MMP-9), as well as proliferation and cell cycle (Cyclin D1), were evaluated by Western blot analysis. As shown in Fig. 6A, stable miR-21-5p knockdown and SET/TAF-Iα overexpression resulted in a significant decrease of MMP-9 and Cyclin D1 in A549 cells, providing further evidence for

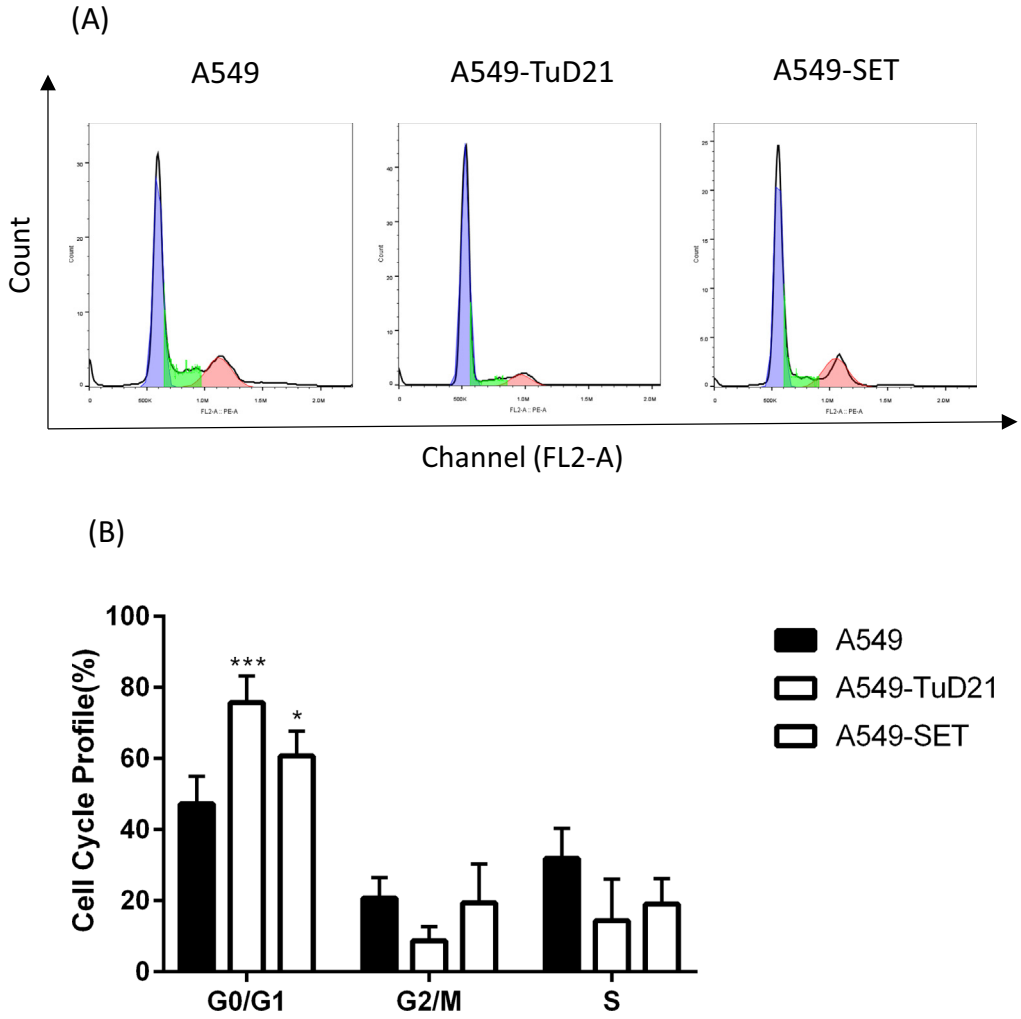

Fig. 5. Stable miR-21-5p knockdown and SET/TAF-Iα overexpression cause cell cycle arrest at G0/G1 phase in A549 cells (A). The data are presented as mean ± SD (B). The experiments were repeated three times, $^{*}p < 0.05$, $^{***}p < 0.001$ compared with A549 cells.

previous observations.

4. Discussion

An increasing body of evidence shows that miRNAs have contradictory functions as oncogenes or tumor suppressors in human cancers based on their specific target genes. The aberrantly expressed SET was also reported in many cancers, such as head and neck squamous carcinoma [22] and ovarian cancer [23]. Hence, the interaction between miRNA and SET is noteworthy and may provide a novel therapeutic strategy for lung cancer treatment. In this study, we first focused on screening for aberrantly expressed SET-targeting miRNAs between normal lung cells and different lung cancer cells, the results of which indicated that miR-21-5p was significantly overexpressed in lung adenocarcinoma cells A549 as compared to lung squamous carcinoma cells and normal lung cells. These observations were consistent with the previous report indicating an increased expression of miR-21-5p in colon adenocarcinoma [24].

Given that foregoing, we believed that the remarkable up-regulation of miR-21-5p could modulate the expression of its target gene SET in A549 cells. Western blot analysis showed for the first time that A549 cells barely express TAF-Iα, a subunit of SET, which agreed with our hypothesis. Studies have shown that SET/TAF-Iβ is more ubiquitous than SET/TAF-Iα; additionally, some cell lines derived from early developmental stages, such as CCRF-CEM, Jurkat, PEER, and NALM-6 cell lines, also lack SET/TAF-Iα expression [25]. Additionally, another study focused on pancreatic cancer indicated that TAF-Iβ is up-regulated in nearly all involved pancreatic cancer cell lines (except AsPC-1) whereas TAF-Iα was markedly increased only in L3.6pl and Capan-1 [26]. Notably, there is currently no report of SET/TAF-Iα expression in lung cancer cells, making the lack of TAF-Iα in A549 cells a novel characteristic with regard to lung adenocarcinoma.

Previous research demonstrated in luciferase assays that miR-199b targets SET in colorectal cancer SW-480 cells [27]; however, evidence for the interaction between miRNA and SET in lung cancer is still lacking. To investigate the correlation we found between SET/TAF-Iα and miR-21-5p, A549-TuD21 cells were constructed before being applied to dual luciferase reporter assays. As a result, we confirmed that miR-21-5p directly bound to SET 3′-UTR in A549 cells.

The mechanisms rendering miR-21-5p pivotal in many cancers are still not fully understood, although it has been reported to be upregulated in many cancers. miR-21-5p is also known to participate in several signaling pathways, such as PPAR [28], PTEN [29] MAPK/ERK and PI3K/AKT [30] that influence tumorigenesis and development in many cancers. Since both miR-21-5p and SET have been described as critical players in cancer progression, we believed that the diverse regulating function of miR-21-5p could also be partially attributed to SET. Our subsequent experiments manifested the distinctly inhibited *in vitro* migration, invasion and proliferation of A549 cells by knockdown of miR-21-5p or overexpression of SET/TAF-Iα, both of which were

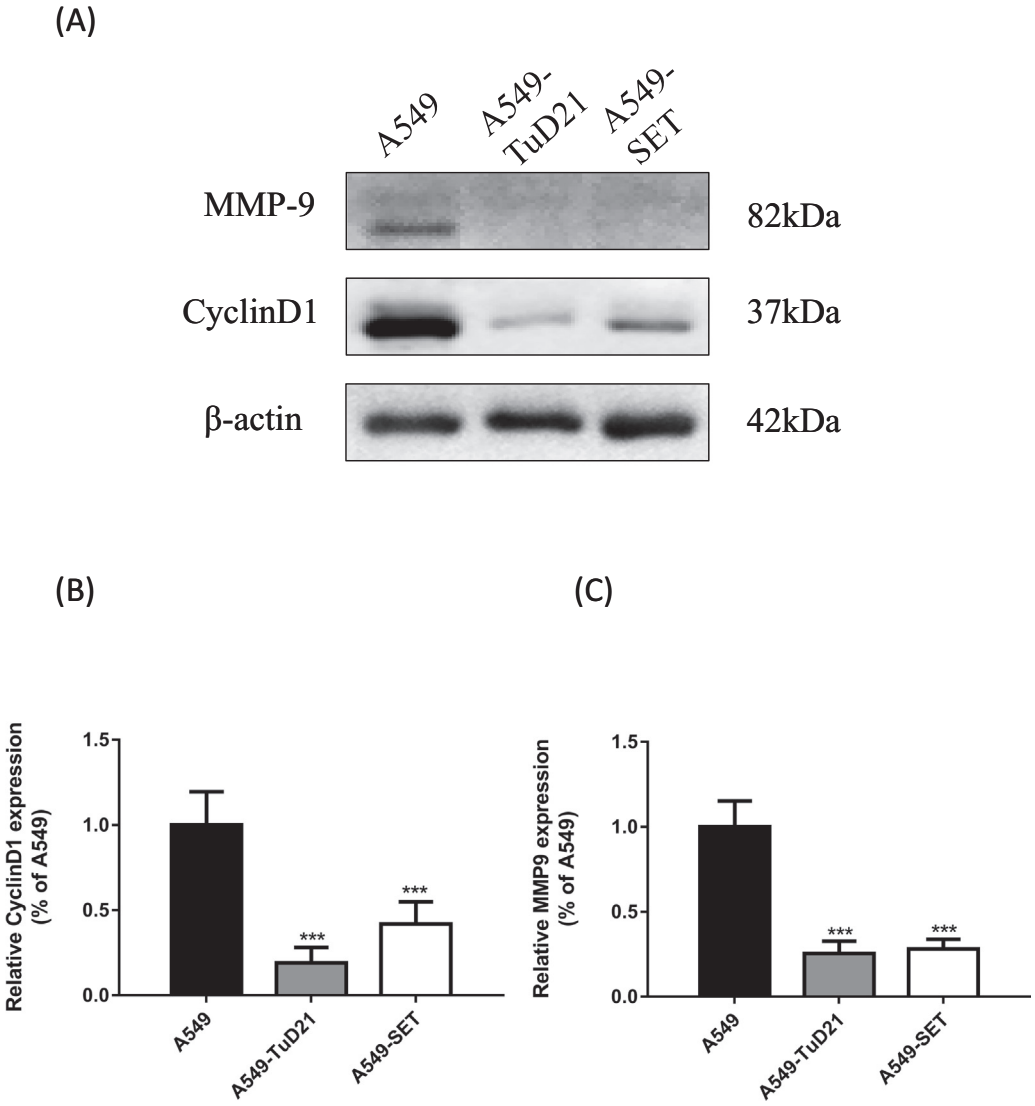

Fig. 6. Representative Western blot (A) and result analysis indicated that stable miR-21-5p knockdown and SET/TAF-Iα overexpression distinctly suppress the endogenous expression of Cyclin D1 (B) and MMP-9 (C) in A549 cells at protein level. All values are expressed as mean ± SD, $^{***}p < 0.001$, and the experiments were repeated three times.

accompanied by elevated SET/TAF-Iα expression. Combined with the results of luciferase reporter assay, the enhanced expression of SET/TAF-Iα in A549-TuD21 could possibly be attributed to the knockdown of miR-21-5p. As expected, our *in vitro* findings are corroborated by the result of our *in vivo* study: both miR-21-5p knockdown and SET/TAF-Iα overexpression suppressed tumor growth of A549 xenografts transplanted into nude mice. The arrest of cell cycle at the G0/G1 phase is frequently related to reduced cell proliferation [31]: we obtained similar results in our cell cycle assay showing that both A549-TuD21 and A549-SET cells accumulated in G0/G1 phase as compared to A549 cells.

It has been suggested that Cyclin D1 plays an important role in cell cycle transition from G0/G1 phase to S phase, cell cycle was found arrested prior to S phase due to the microinjection of antisense plasmids or antibodies to Cyclin D1 [32]. A recent study also indicated that downregulation of Cyclin D1 could account for the G0/G1 phase arrest in TYL-treated VSMC [33]. Moreover, in epithelial ovarian cell (EOC cell), cyclin D1 was found to be an important proliferation regulator in the mechanism of action of miR-211, and closely related to xenograft tumor growth [34]. MMP-9 (matrix metalloproteinase-9) is associated with the degradation of extracellular matrix and thus promotes the essential steps for tumor metastasis, namely cancer cell invasion and migration [35]. Up-regulation of MMP-9 was found related to worse overall survival among colorectal cancer patients, by comparing those with down-regulated MMP-9 expression [36]. To explore the relevant mechanisms whereby miR-21-5p or SET/TAF-Iα could play a role on these oncogenic functions, we used Western blot analysis to evaluate the expression of Cyclin D1 and MMP-9, both of which were found to be significantly inhibited in A549-TuD21 and A549-SET cells. Although our results were consistent with the above reports, the exact mechanism of action of miR-21 or SET/TAF-Iα on Cyclin D1 and MMP-9 is yet unknown, and it is clear that other downstream targets could jointly play a role.

In spite of the strong homology between TAF-Iα and TAF-Iβ, the first 37 different amino acids could possibly contribute to the contradictory effect of SET, although the biological functions of TAF-Iβ were well explored, few studies have focused on TAF-Iα. Here, for the first time we hypothesized that the overexpression of SET/TAF-Iα might also suppress tumor progression of lung adenocarcinoma. Unexpectedly, the expression of SET/TAF-Iβ in A549-SET cells was significantly reduced. Given that the potential correlations between isoform length and cell migration have been pointed to in several studies – for example, the most aggressive basal breast cancer type, has the highest ratio of short

RECK to long RECK [37] — we hypothesize that the expression of SET/TAF-Iα might also change the way through which SET was alternatively spliced, thus decreasing the expression of SET/TAF-Iβ and inhibiting tumor cell migration.

In summary, this study demonstrates that both *in vitro* and *in vivo*, either overexpression of SET/TAF-Iα or knockdown of miR-21-5p, inhibits the oncogenic function of A549 cells, which improves our understanding that miR-21-5p might promote lung cancer progression partially through targeting SET/TAF-Iα. Based on all of the above evidence, the interaction between miR-21-5p and SET/TAF-Iα may provide a valuable insight for in-depth research of lung cancer therapy.

Declaration of Competing Interest

The authors do not have any conflicts of interest or financial interests to disclose.

Acknowledgment

This work was supported by the National Natural Science Foundation of China (NSFC) [81872666], Shenzhen Basic Research Plan [JCYJ20160428142316603], Sanming Project of Medicine in Shenzhen [SZSM201611090], and Shenzhen Municipal Government of China [JCYJ20160328161613864, JSGG20170414104216477].

References

[1] D.R. Youlden, S.M. Cramb, P.D. Baade, The International Epidemiology of Lung Cancer: geographical distribution and secular trends, J. Thorac. Oncol. (2008) 819–831.
[2] R.L. Siegel, K.D. Miller, A. Jemal, Cancer statistics, 2019, CA Cancer J. Clin. (2019) 7–34.
[3] C. Moran, Importance of molecular features of non-small cell lung cancer for choice of treatment, Am. J. Pathol. (2011) 1940–1948.
[4] J. Subramanian, R. Govindan, Molecular profile of lung cancer in never smokers, EJC Suppl. (2013) 248–253.
[5] M. Von Lindern, S. Van Baal, J. Wiegant, et al., Can, a putative oncogene associated with myeloidleukemogenesis, may be activated by fusion of its 3′ half to different genes: characterization of the set gene, Mol. Cell. Biol. (1992) 3346–3355.
[6] M. Li, A. Makkinje, Z. Damuni, The myeloid leukemia-associated protein SET is a potent inhibitor of protein phosphatase 2A, J. Biol. Chem. (1996) 11059–11062.
[7] K. Nagata, H. Kawase, H. Handa, et al., Replication factor encoded by a putative oncogene, set, associated with myeloid leukemogenesis, Proc. Natl. Acad. Sci. U. S. A. (1995) 4279–4283.
[8] A. Kalousi, A.S. Hoffbeck, P.N. Selemenakis, et al., The nuclear oncogene SET controls DNA repair by KAP1 and HP1 retention to chromatin, Cell Rep. (2015) 149–163.
[9] J.P. Chambon, S.A. Touati, S. Berneau, et al., The PP2A inhibitor I2PP2A is essential for sister chromatid segregation in oocyte meiosis II, Curr. Biol. (2013) 485–490.
[10] J.Y. Kim, K.S. Lee, J.E. Seol, et al., Inhibition of p53 acetylation by INHAT subunit SET/TAF-Iβ represses p53 activity, Nucleic Acids Res. (2012) 75–87.
[11] K. González-Arzola, I. Díaz-Moreno, A. Cano-González, et al., Structural basis for inhibition of the histone chaperone activity of SET/TAF-Iβ by cytochrome c, Proc. Natl. Acad. Sci. U. S. A. (2015) 9908–9913.
[12] M. Janghorban, A.S. Farrell, B.L. Allen-Petersen, et al., Targeting c-MYC by antagonizing PP2A inhibitors in breast cancer, Proc. Natl. Acad. Sci. U. S. A. (2014) 9157–9162.
[13] A.S. Farrell, B. Allen-Petersen, C.J. Daniel, et al., Targeting inhibitors of the tumor suppressor PP2A for the treatment of pancreatic cancer, Mol. Cancer Res. (2014) 924–939.
[14] S.A. Saddoughi, S. Gencer, Y.K. Peterson, et al., Sphingosine analogue drug FTY720 targets I2PP2A/SET and mediates lung tumour suppression via activation of PP2A-RIPK1-dependent necroptosis, EMBO Mol. Med. (2013) 105–121.
[15] K. Plaisance-Bonstaff, R. Renne, Viral miRNAs, Methods Mol. Biol. (2011) 43–66.
[16] M. Chekulaeva, W. Filipowicz, Mechanisms of miRNA-mediated post-transcriptional regulation in animal cells, Curr. Opin. Cell Biol. (2009) 452–460.
[17] M.T. Landi, Y. Zhao, M. Rotunno, et al., MicroRNA expression differentiates histology and predicts survival of lung cancer, Clin. Cancer Res. (2010) 430–441.
[18] L. Yu, N.W. Todd, L. Xing, et al., Early detection of lung adenocarcinoma in sputum by a panel of microRNA markers, Int. J. Cancer (2010) 2870–2878.
[19] H.B. Bian, X. Pan, J.S. Yang, et al., Upregulation of microRNA-451 increases cisplatin sensitivity of non-small cell lung cancer cell line (A549), J. Exp. Clin. Cancer Res. (2011) 20.
[20] H. Jin, M. Yu, Y. Lin, et al., Mir-502-3P suppresses cell proliferation, migration, and invasion in hepatocellular carcinoma by targeting SET, Onco. Targets Ther. (2016) 3281–3289.
[21] T. Haraguchi, Y. Ozaki, H. Iba, Vectors expressing efficient RNA decoys achieve the long term suppression of specific microRNA activity in mammalian cells, Nucleic Acids Res. (2009) e43.
[22] L.M. Sobral, L.O. Sousa, R.D. Coletta, et al., Stable SET knockdown in head and neck squamous cell carcinoma promotes cell invasion and the mesenchymal-like phenotype in vitro, as well as necrosis, cisplatin sensitivity and lymph node metastasis in xenograft tumor models, Mol. Cancer (2014) 32.
[23] V. Ouellet, C. Le Page, M.C. Guyot, et al., SET complex in serous epithelial ovarian cancer, Int. J. Cancer (2006) 2119–2126.
[24] W. Yu, K. Zhu, Y. Wang, et al., Overexpression of miR-21-5p promotes proliferation and invasion of colon adenocarcinoma cells through targeting CHL1, Mol. Med. (2018) 36.
[25] K. Nagata, S. Saito, M. Okuwaki, et al., Cellular localization and expression of template-activating factor I in different cell types, Exp. Cell Res. (1998) 274–281.
[26] H.R. Mody, S.W. Hung, K. Naidu, et al., SET contributes to the epithelial-mesenchymal transition of pancreatic cancer, Oncotarget (2017) 67966–67979.
[27] I. Cristóbal, C. Caramés, R. Rincón, et al., Downregulation of microRNA-199b predicts unfavorable prognosis and emerges as a novel therapeutic target which contributes to PP2A inhibition in metastatic colorectal cancer, Oncotarget (2017) 40169–40180.
[28] J. Liu, H. Li, L. Sun, et al., Epigenetic alternations of MicroRNAs and DNA methylation contribute to liver metastasis of colorectal cancer, Dig. Dis. Sci. (2019) 1523–1534.
[29] G. Zhu, X. Liu, H. Li, et al., Kaempferol inhibits proliferation, migration, and invasion of liver cancer HepG2 cells by down-regulation of microRNA-21, Int. J. Immunopathol. Pharmacol. (2018) 2058738418814341.
[30] Q. Zhao, S. Chen, Z. Zhu, et al., miR-21 promotes EGF-induced pancreatic cancer cell proliferation by targeting Spry2, Cell Death Dis. (2018) 1157.
[31] X. Yang, L. Zhao, T. Zhang, et al., Protosappanin B promotes apoptosis and causes G1 cell cycle arrest in human bladder cancer cells, Sci. Rep. (2019) 1048.
[32] V. Baldin, J. Lukas, M.J. Marcote, et al., Cyclin D1 is a nuclear protein required for cell cycle progression in G1, Genes Dev. (1993) 812–821.
[33] H. Joa, T. Blažević, C. Grojer, et al., Tylophorine reduces protein biosynthesis and rapidly decreases cyclin D1, inhibiting vascular smooth muscle cell proliferation in vitro and in organ culture, Phytomedicine (2019) 152938, , https://doi.org/10.1016/j.phymed.2019 (Epub ahead of print).
[34] B. Xia, S. Yang, T. Liu, G. Lou, et al., miR-211 suppresses epithelial ovarian cancer proliferation and cell-cycle progression by targeting cyclin D1 and CDK6, Mol. Cancer (2015) 57.
[35] M. Egeblad, Z. Werb, New functions for the matrix metalloproteinases in cancer progression, Nat. Rev. Cancer (2002) 161–174.
[36] X.Z. Yang, S.Z. Cui, L.S. Zeng, et al., Overexpression of Rab1B and MMP-9 predicts poor survival and good response to chemotherapy in patients with colorectal cancer, Aging (Albany NY) (2017) 914–929.
[37] H.N. Lee, M. Mitra, O. Bosompra, RECK isoforms have opposing effects on cell migration, Mol. Biol. Cell (2018) 1825–1838.